

Inhibition of Cyclin-Dependent Kinase Activity and Induction of Apoptosis by Preussin in Human Tumor Cells

TATJANA V. ACHENBACH,¹ EMILY P. SLATER,¹ HARM BRUMMERHOP,²
THORSTEN BACH,² AND ROLF MÜLLER^{1*}

*Institute of Molecular Biology and Tumor Research, Department of Medicine,¹ and
Department of Chemistry,² Philipps University, Marburg, Germany*

Received 14 February 2000/Returned for modification 17 July 2000/Accepted 21 July 2000

In this paper, we report that (+)-preussin, a pyrrolidinol alkaloid originally identified as an antifungal agent, has growth-inhibitory and cytotoxic effects on human cancer cells. Preussin was found to be a potent inhibitor of cyclin E kinase (CDK2-cyclin E) in vitro (50% inhibitory concentration; ~500 nM) and to inhibit cell cycle progression into S phase. In agreement with these findings, the level of the cyclin-dependent kinase inhibitor p27^{KIP-1} is increased in response to preussin treatment while the expression of both cyclin A and the transcription factor E2F-1 is down-regulated. Preussin also induces programmed cell death (apoptosis), which requires caspase activation and involves the release of cytochrome *c* from mitochondria. This induction of apoptosis is not blocked by high levels of Bcl-2, which usually confers resistance to chemotherapeutic agents. Taken together, our data indicate that preussin could be a promising lead compound for the development of a new class of potent antitumor drugs.

Most of the drugs currently used in anticancer therapy kill target cells by triggering programmed cell death. This frequently involves the induction of apoptosis, a process characterized by distinct systematic morphological changes, including a decrease in cell volume, chromatin condensation, DNA fragmentation, cell surface blebbing, and the formation of membrane-bound apoptotic bodies. A major problem with conventional chemo- and radiotherapy is the fact that tumor cells usually evolve potent antiapoptotic mechanisms that counteract the induction of death in response to treatment (34). This can be due to the selection pressure imposed by proapoptotic oncogenic alterations that accumulate during tumor development or, in relapsed cancers, result from the selection of treatment-resistant variants. Therefore, the identification of novel drugs that are refractory to the antiapoptotic mechanisms employed by tumor cells has a high priority.

An essential step in apoptosis is the activation of caspases, cysteine proteases that are synthesized as inactive proenzymes and, after activation, cleave specific substrates at aspartic acid residues (43). Two different pathways have been partly characterized to date. The first is triggered by the release of cytochrome *c* from mitochondria, often in a p53-dependent manner in response to DNA damage (9). Cytochrome *c* then enables the assembly of a cytoplasmic multiprotein complex, the apoptosome. Consequently, caspase 9 is activated which, in turn, leads to the activation of the executioner caspase, caspase 3. The second pathway is triggered by death receptors of the tumor necrosis factor alpha receptor family, such as TNFR, Fas (CD95), or TRAIL (9). The ligand-mediated clustering of these receptors results in the assembly of the membrane-associated death initiation signaling complex, which involves the activation of caspase 8, followed by the activation of caspase 3. This pathway can also branch off to the mitochondrial pathway through the caspase 8-mediated cleavage of a proapoptotic member of the Bcl-2 family, Bid, which can trigger the release

of cytochrome *c* from mitochondria. Defects counteracting the apoptosis-inducing potency of antitumor drugs can occur at multiple steps in diverse ways. Important examples are the loss of p53 (25) and the expression of antiapoptotic members of the Bcl-2 family (27, 33).

Apoptosis is induced not only by death receptor agonists or agents that cause DNA damage, mitotic spindle dysfunction, or metabolic perturbations but also by interference with coordinated cell cycle progression. For example, the deregulated expression of proto-oncogenes such as c-Myc, in conjunction with an unphysiological cell cycle block, is incompatible with the cell's survival (14, 20). Likewise, the inhibition of cyclin-dependent kinases (CDKs)—the enzymes driving progression through the cell cycle—triggers programmed cell death in tumor cells (1, 4, 5, 8, 10, 30, 31, 36, 40). These and other observations have laid the foundation for the definition of a new class of antitumor agents that function by direct interference with cell cycle regulatory processes (15–17, 35). One of the prototypes of this class of compounds is the CDK inhibitor flavopiridol (FP) (13, 24, 28), which has shown promising tumor response in preclinical models (1, 4, 10, 12, 30, 31, 36, 40) and is currently undergoing clinical trials (39, 45).

In an effort to identify new drugs with improved antitumor properties, we found that the pyrrolidinol alkaloid (+)-preussin (L-657,398), originally found in fermentation of *Aspergillus ochraceus* and *Preussia* sp. as a broad-spectrum antifungal agent active against both yeast and filamentous fungi (22, 23, 38), has potent growth-inhibitory and apoptosis-inducing effects on human cancer cells. Preussin is structurally related to the protein synthesis inhibitor anisomycin (22, 38) (Fig. 1), but its relatively weak effect on translation, seen in the present study, suggests that the crucial target of preussin is different. Surprisingly, we found that preussin is a potent inhibitor of cyclin E kinase (CDK2-cyclin E) in vitro, which explains its ability to inhibit cell cycle progression through G₁. Preussin also induces apoptosis, which involves the release of cytochrome *c* and the activation of caspases 3 and 8. Preussin also induces apoptosis in tumor cells, which express high levels of Bcl-2, and this distinguishes preussin from clinically used chemotherapeutic agents such as doxorubicin (Dox), etoposide

* Corresponding author. Mailing address: Institut für Molekularbiologie und Tumorforschung (IMT), Philipps-Universität, Emil-Mannkopf-Str. 2, 35033 Marburg, Germany. Phone: 49-6421-2866236. Fax: 49-6421-2868923. E-mail: mueller@imt.uni-marburg.de.

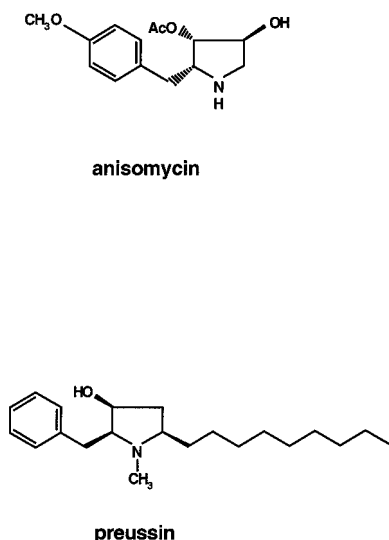


FIG. 1. Chemical structures of anisomycin and preussin. AcO, acetyloxy.

(Etop), camptothecin (Cam), cisplatin (Cispl), and 5'-fluorouracil (5' FU). Preussin might therefore provide an interesting lead structure for the design of novel antitumor drugs.

MATERIALS AND METHODS

Chemicals. Fetal bovine serum, horseradish peroxidase-conjugated goat anti-mouse immunoglobulin G, dithiothreitol (DTT): aprotinin, leupeptin, Cam, Dox, Etop, Cispl, 5'FU, and anisomycin were purchased from Sigma (Deisenhofen, Germany). Mouse monoclonal anti-human p27^{kip}, poly(ADP-ribose) polymerase (PARP), and anti-caspase 3 (CPP32) antibodies were from Transduction Laboratories Dianova (Hamburg, Germany). The cytochrome *c* antibody was purchased from Pharmingen (Hamburg, Germany), the mouse monoclonal antiactin antibody was from Roche (Mannheim, Germany), and the caspase 8, E2F-1, and cyclin A antibodies were from Santa Cruz (Heidelberg, Germany). The ECL immunoblot analysis reagents were obtained from Amersham Life Science, Inc. (Braunschweig, Germany); ATP was from Pharmacia Biotech Europe (Brussels, Belgium); and the caspase inhibitor zVAD-fmk was from Stratagene (Heidelberg, Germany). The annexin V kit was purchased from Nexins Research B.V. (Kattendijke, The Netherlands). FP was kindly provided by H.-H. Sedlacek (Aventis-Pharma, Marburg, Germany), and recombinant CDK2 kinase was provided by D. Müller and M. Eilers (Institute of Molecular Biology and Tumor Research, Marburg, Germany). Preussin was synthesized as previously described (3).

Cell lines and cell culture. The HeLa (ATCC CCL-2), A549 (ATCC CCL-185; obtained from K. Havemann, Marburg, Germany), MeWo (18) (provided by I. Hart, London, England), and MCF-7 (ATCC HTB-22; obtained from G. Emons, Göttingen, Germany) cell lines were cultured in Dulbecco's modified Eagle medium. The medium for MCF-7 cells was supplemented with 0.9 mg of insulin per ml. HL-60 cells (ATCC CCL-240), the lung carcinoma cell lines SW2 and H69 (46) (both provided by U. Zangemeister-Wittke, Zürich, Switzerland), and the prostate carcinoma cell lines PC-3 (ATCC CRL-1435), DU-145 (ATCC HTB-81), and LNCaP (ATCC CRL-1740) (all three were provided by G. Aumüller, Marburg, Germany) were cultured in RPMI 1640 medium. Both media were supplemented with 10% fetal bovine serum, 100 U of penicillin ml⁻¹, and 100 µg of streptomycin ml⁻¹. All cells were maintained in culture at 37°C with 5% CO₂ in a humidified incubator. Preussin, FP, Cam, 5'FU, Dox, Etop, Cispl, anisomycin, and zVAD-fmk were dissolved in dimethyl sulfoxide and added to the culture medium at the concentrations indicated. The final concentration of dimethyl sulfoxide in the medium was less than 1% (vol/vol). Cells were incubated at 37°C and harvested at the time points indicated in the figures.

Cytotoxicity assay. Cells were seeded in microtiter plates at 30,000 per well. Sixteen hours later, different concentrations of preussin were added for 48 h. After an additional 48 h in normal medium, cells were stained with crystal violet (6) and the retained dye was measured using an enzyme-linked immunosorbent assay reader at a wavelength of 540 nm. Wells containing cells with medium alone were used as a negative control. Each experiment was performed using four replicate wells for each drug concentration, and three independent experiments were carried out for each cell line. Cell survival was calculated as (absorbance of wells containing drug/absorbance in drug-free wells) × 100. The 50% inhibitory concentration (IC₅₀) was defined as the drug concentration giving 50%

of maximal absorbance in each test and was determined graphically from dose-response curves.

[³⁵S]methionine incorporation. For metabolic labeling, the cells were incubated with different concentrations of preussin or anisomycin for 18 h. For the last 2 h, the cells were incubated in 200 µl of L-methionine-free RPMI 1640 medium containing 7.5 µCi of [³⁵S]methionine. The cells were washed with medium, and cell extracts were prepared as described above. Trichloroacetic acid was added to each sample to a final concentration of 10%, and the mixture was incubated for 10 min on ice to precipitate the proteins. Subsequently, the samples were centrifuged, the pellets were resuspended in 50 µl of 0.1 M NaOH, and after addition of 3 ml of Rotiszint scintillation fluid (Carl Roth, GmbH & Co., Karlsruhe, Germany), the radioactivity was counted in a scintillation counter (Beckman, Munich, Germany).

Flow cytometric analysis. Cells were harvest from a 10-cm-diameter dish, washed two times with phosphate-buffered saline (PBS), and fixed for 1 h in ice-cold 75% ethanol. Following fixation, the cells were resuspended in PBS and incubated with RNase A (50 µg ml⁻¹) and the DNA was stained with propidium iodide (50 µg ml⁻¹). Flow cytometric analysis was performed on a FACStarPlus or a FACSCalibur (Becton Dickinson, Heidelberg, Germany). The DNA distribution for cell cycle analysis was determined with the CellFit program or by manual gating. For annexin V staining (see Fig. 7C), cells were washed twice with PBS and resuspended in 1 × binding buffer (Nexins Research). Subsequently, 5 µl of fluorescein isothiocyanate-labeled annexin V (Nexins Research) and propidium iodide to a final concentration of 2 µg ml⁻¹ were added to the cells. After a 15-min incubation on ice, the cells were analyzed on a FACStarPlus as recommended by the manufacturer.

Kinase assay. Recombinant CDK2-cyclin E kinase was overexpressed in Sf9 cells and purified as previously described (29). Recombinant protein (20 ng in 1 µl) was mixed with 18 µl of kinase buffer (10 mM MnCl₂, 10 mM MgCl₂, 10 mM KCl, 20 mM HEPES [pH 7.3], 5 µg of leupeptin ml⁻¹, 5 µg of aprotinin ml⁻¹, 100 µM β-glycerophosphate, 5 µM phenylmethylsulfonyl fluoride, 1 mM DTT, and 1 µM NaF), 1.25 µl of 1 mM histone H1, and 1.25 µl of 1 mM ATP. The mixture was preincubated in the absence or presence of different concentrations of FP, Cam, anisomycin, or preussin at 37°C for 30 min. Following the addition of 0.25 µl of [γ-³²P]ATP (10 µCi µl⁻¹), the mixture was incubated at 30°C for 30 min. The reaction was stopped by the addition of 10 × sodium dodecyl sulfate (SDS) loading buffer (2). Proteins were separated on a 12% SDS-polyacrylamide gel, and the ³²P-labeled histone H1 was visualized on Kodak BIOMAX film.

Preparation of cell extracts. Cells were harvested from 10-cm-diameter plates, washed twice in PBS, and resuspended in an equal volume of buffer containing 20 mM HEPES (pH 7.8), 450 mM NaCl, 0.2 mM EDTA, 25% glycerol, 5 µM DTT, 5 µM phenylmethylsulfonyl fluoride, 0.5 µg of leupeptin ml⁻¹, and 5 µg of aprotinin ml⁻¹. The cells were incubated for 5 min on ice and then lysed by three freeze-thaw cycles (freezing in liquid nitrogen and thawing in a 30°C water bath). The lysate was centrifuged at 13,000 × g for 10 min at 4°C, and the supernatant was stored at -80°C.

Immunoblot analysis. Samples of control and treated cells were separated by SDS-polyacrylamide gel electrophoresis and transferred onto nitrocellulose membranes by electroblotting. The membrane was blocked with 5% nonfat milk for 2 h and incubated with the primary antibody for 2 h at room temperature. Unbound antibody was removed by washing with PBS five times for 4 min each. The membrane was then incubated with the secondary antibody (alkaline phosphatase conjugate; Santa Cruz, Heidelberg, Germany) for 2 h at room temperature and washed, and the enzyme was detected upon addition of the ECL reagents (Amersham Pharmacia Biotech).

Morphological evaluation of apoptosis. Cells were stained with Hoechst 33342 (10 µM) and propidium iodide (10 µM) for 10 min and analyzed under a fluorescence microscope (Leitz Aristoplan) with excitation at 360 nm. Because Hoechst 33342 stains all nuclei and propidium iodide stains nuclei of cells with a disrupted plasma membrane, nuclei of viable, necrotic, and apoptotic cells could be distinguished as blue round nuclei, pink round nuclei, and fragmented blue or pink nuclei, respectively (42).

Isolation of low-molecular-weight chromosomal DNA. HL-60 cells were cultured in RPMI medium and treated with preussin at different concentrations for 24 h. The cells were collected by centrifugation, and the pellet was resuspended in 300 µl of lysis buffer (10 mM Tris-HCl [pH 7.5], 10 mM EDTA [pH 8], 0.2% Triton X-100) and incubated at room temperature for 10 min. After addition of 10 µl of RNase A (10 mg ml⁻¹), the DNA was incubated at 37°C for 1 h. Following addition of 10 µl of proteinase K (20 mg ml⁻¹), incubation was continued at 55°C for 8 to 18 h. The DNA was extracted using phenol and phenol-chloroform-isoamyl alcohol (25:24:1) solutions and then ethanol precipitated. The pellet was dissolved in 20 µl of TE buffer (10 mM Tris-HCl [pH 7.9], 1 mM EDTA). The DNA fragments present in 5 to 10 µl of the aliquots were fractionated on a 2% agarose gel and visualized using ethidium bromide.

Preparation of cytosolic extracts (7). HL-60 cells were collected by centrifugation at 800 rpm for 5 min at 4°C. The cells were washed twice with ice-cold PBS (pH 7.4) and then centrifuged. The pellet was resuspended in 400 µl of extraction buffer containing 288 mM sucrose: 50 mM piperazine-N,N'-bis(2-ethanesulfonic acid) [PIPES]-KOH [pH 7.4], 50 mM KCl, 5 mM EGTA; 2 mM MgCl₂, 1 mM DTT, and protease inhibitors (see preparation of protein extracts). After a 30-min incubation on ice, cells were spun at 10,000 × g for 15 min and the

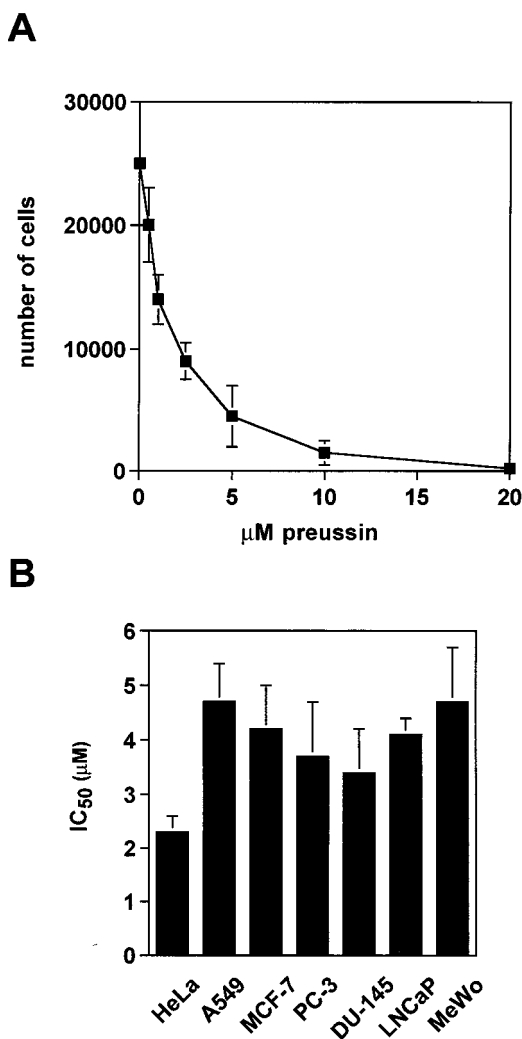


FIG. 2. Inhibition by preussin of human cancer cell growth. (A) Dose-dependent inhibition of HL-60 cell growth. Cells were incubated with increasing concentrations of preussin for 18 h. The number of remaining live cells was determined and plotted as a function of the drug concentration. (B) IC_{50} s for different human tumor cell lines. Cells were grown in microtiter plates, treated with preussin at increasing concentrations for 48 h, washed with PBS, reseeded with normal medium, and allowed to grow for another 48 h before staining with crystal violet. The dye remaining was measured in an enzyme-linked immunosorbent assay reader at 540 nm, and the IC_{50} s were calculated as described in Materials and Methods.

supernatants were removed and stored at -80°C until analysis by gel electrophoresis.

RESULTS

Growth inhibition of human cancer cells by preussin. Since growth-inhibitory properties have been described for anisomycin, we sought to investigate whether the structurally related compound preussin might share these properties. As shown in Fig. 2A, treatment of the human promyelocytic leukemia cell line HL-60 with increasing concentrations of preussin led to a dose-dependent decrease in the live-cell counts with IC_{50} of 1.2 μM after 18 h of treatment. A similar range of IC_{50} s was obtained with preussin treatment of seven other human carcinoma cell lines, as detected by a microtiter plate-based crystal violet assay (Fig. 2B). IC_{50} s ranging from 2.3 to 4.5 μM after 48 h of treatment were determined for the cervical carcinoma

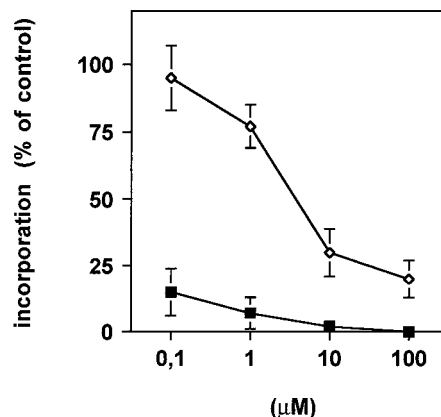


FIG. 3. Incorporation of [^{35}S]methionine by A549 cells exposed to increasing concentrations of anisomycin (■) or preussin (◇).

cell line HeLa; the lung adenocarcinoma cell line A549; the breast carcinoma cell line MCF-7; the three prostate carcinoma cell lines PC-3, DU-145, and LNCaP; and the melanoma cell line MeWo. In general, low concentrations of preussin seemed to inhibit cell proliferation while higher concentrations resulted in cell death. For instance, following a 1-week treatment of HL-60 cells with preussin, cultures were incubated in normal growth medium. There was no recovery of cell growth after exposure to 1 μM preussin, but cells treated with a 200 nM concentration of the drug resumed growth (data not shown).

Effect on protein biosynthesis. As preussin is structurally related to the translational inhibitor anisomycin, we investigated whether its growth-inhibitory effects could be ascribed to blockage of protein synthesis. Therefore, metabolic labeling of HL-60 cells by [^{35}S]methionine incorporation was performed in the presence of different concentrations of either drug. As can be seen in Fig. 3, preussin inhibited the incorporation of [^{35}S]methionine into cellular protein but its inhibitory potential was about 3 orders of magnitude lower than that of anisomycin (26). At concentrations at which preussin efficiently induced cell death (~ 5 μM), the inhibition of protein synthesis was $\sim 50\%$. In the case of other protein synthesis inhibitors, cytotoxic effects have been seen only when protein synthesis was reduced to $<10\%$ of the normal level. It is therefore unlikely that the observed growth-inhibitory and cytotoxic effects of preussin can be attributed to inhibition of protein biosynthesis.

Inhibition of cell cycle progression into S phase. As the inhibition of cell growth by preussin does not seem to be due to inhibition of protein synthesis, we asked whether preussin might inhibit progression through the cell cycle. As determined by fluorescence-activated cell sorter (FACS) analysis of Hoechst 33258-stained cells, an 18-h treatment of A549 cells with 5 μM preussin led to an increase in the G_1 fraction from 64% (untreated cells) to 88% (Fig. 4A). Analysis of the DNA distribution in other human carcinoma cell lines treated with concentrations of preussin greater than 500 nM showed a similar accumulation of cells in the G_1 phase (data not shown). With HL-60 cells, an enlarged population of G_1 cells was also seen after preussin treatment but even more conspicuous was the dramatic increase in hypodiploid (sub- G_1) cells (Fig. 4B), which is indicative of apoptosis. The hypodiploid fraction increased from 12% in control cells to 33 and 89% in cells treated with 1 and 5 μM preussin, respectively. This marked

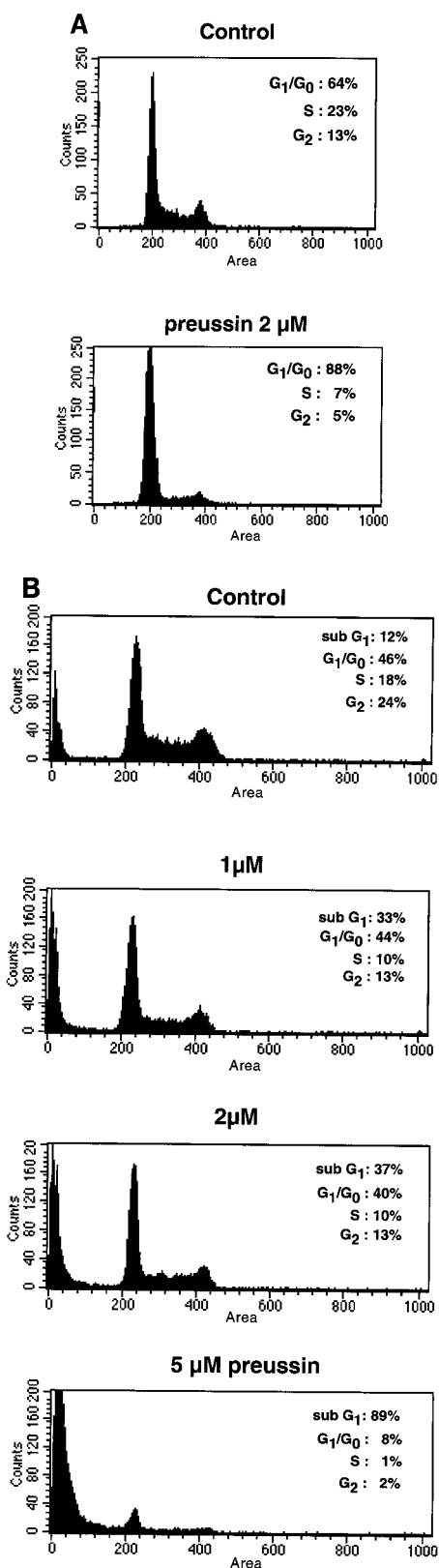


FIG. 4. Cell cycle distribution of A549 (A) and HL-60 (B) cells before and after 18 h of treatment with preussin.

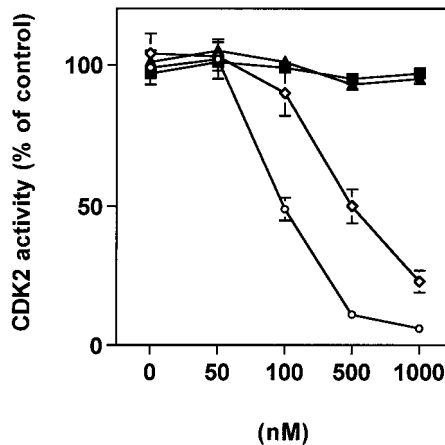


FIG. 5. Inhibition of CDK2 activity by preussin in vitro. The activity of recombinant cyclin E-CDK2 was measured in the presence of increasing concentrations of preussin (◇), FP (○), anisomycin (■), or Cam (▲).

cytotoxic effect in HL-60 cells is presumably due to the fact that HL-60 cells are particularly sensitive to the induction of cell death. This is also suggested by the relatively high number of dead cells in the untreated cell population (12% sub-G₁ cells in Fig. 4B). Taken together, these results suggest that a delay or arrest of cell cycle progression through G₁ into S phase, as well as the induction of cell death, contributes to the growth-inhibitory properties of preussin described above (Fig. 2).

Inhibition of cyclin E kinase by preussin in vitro. In view of its effects on the cell cycle, we sought to investigate whether preussin might be able to directly modulate the activity of cyclin E-CDK2, a protein kinase that plays a crucial role in controlling the entry into S phase. For this purpose, we used the purified recombinant holoenzyme expressed from a baculovirus vector and tested the effect of preussin in an in vitro kinase assay. As shown in Fig. 5, preussin strongly inhibited cyclin E kinase activity (IC₅₀, ~500 nM). FP, a particularly potent general inhibitor of CDKs (13) was used as a positive control (IC₅₀, ~100 nM). Anisomycin and the topoisomerase inhibitor Cam had no effect on CDK2 activity. These data show that preussin is a direct and potent inhibitor of cyclin E-CDK2 kinase, which is in perfect agreement with the inhibitory effect on G₁-to-S progression described above (Fig. 4).

Effect of preussin on expression of cell cycle regulatory proteins. To confirm and extend the conclusions regarding preussin's effect on cell cycle progression, we analyzed the expression of three different proteins involved in the control of the cell cycle (41, 47): (i) the CDK inhibitor p27^{KIP-1}, which accumulates in G₀/G₁-arrested cells owing to protein stabilization; (ii) E2F-1, whose expression is up-regulated in late G₁/early S phase due to the dissociation of the retinoblastoma protein (pRb)-E2F repressor complexes; and (iii) cyclin A, which is also up-regulated in late G₁/early S phase by E2F released from pRb complexes. Immunoblot assays were performed with extracts from untreated and preussin-treated proliferating A549 and HL-60 cells using p27-, E2F-1-, and cyclin A-specific antibodies. Actin served as a control to exclude unspecific effects on protein synthesis. In addition, A549 cells synchronized in G₁ by density arrest were included for comparison. The data in Fig. 6 clearly support the conclusion that preussin inhibits cell cycle progression into S phase. As expected, the preussin-treated cells showed accumulation of p27^{KIP-1} and decreased expression of both E2F-1 and cyclin A. The observed increase in p27^{KIP-1} levels is also in perfect agreement

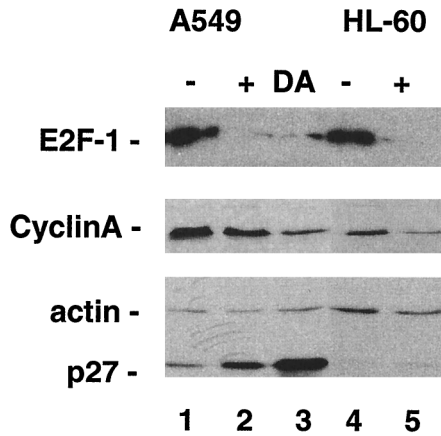


FIG. 6. Effect of preussin on the expression of the cell cycle regulators cyclin A, E2F-1, and p27 in A549 and HL-60 cells. Lanes: -, untreated cells; +, cells exposed to preussin for 18 h; DA, density arrested.

with the inhibition of cyclin E-CDK2 by preussin, since the phosphorylation by cyclin E kinase targets p27 for proteolytic degradation (41). The very low expression of p27^{KIP-1} in HL-60 cells is probably due to the specific growth behavior of these nonadherent leukemia cells.

Induction of apoptosis by preussin. Next, we investigated the mechanism of preussin-induced cell death in further detail. Treatment of HL-60 cells with increasing concentrations of preussin led to fast and progressive induction of apoptosis, as determined by Hoechst 33342-propidium iodide staining of the cells (Fig. 7A). Generally, the cells displayed punctate Hoechst 33342 staining characteristic of the chromatin condensation that accompanies apoptosis. Staining by propidium iodide was indicative of a compromised membrane, which is characteristic of necrotic cells and late stages of apoptosis. Cell killing by preussin ranged from 27% at a concentration of 0.5 μM preussin to 80% at 5 μM after 18 h (Fig. 7A).

To obtain further evidence that the process leading to cell death in preussin-treated cells is indeed apoptosis, we studied two additional characteristic features of apoptosis: internucleosomal DNA cleavage and exposure of phosphatidylserine

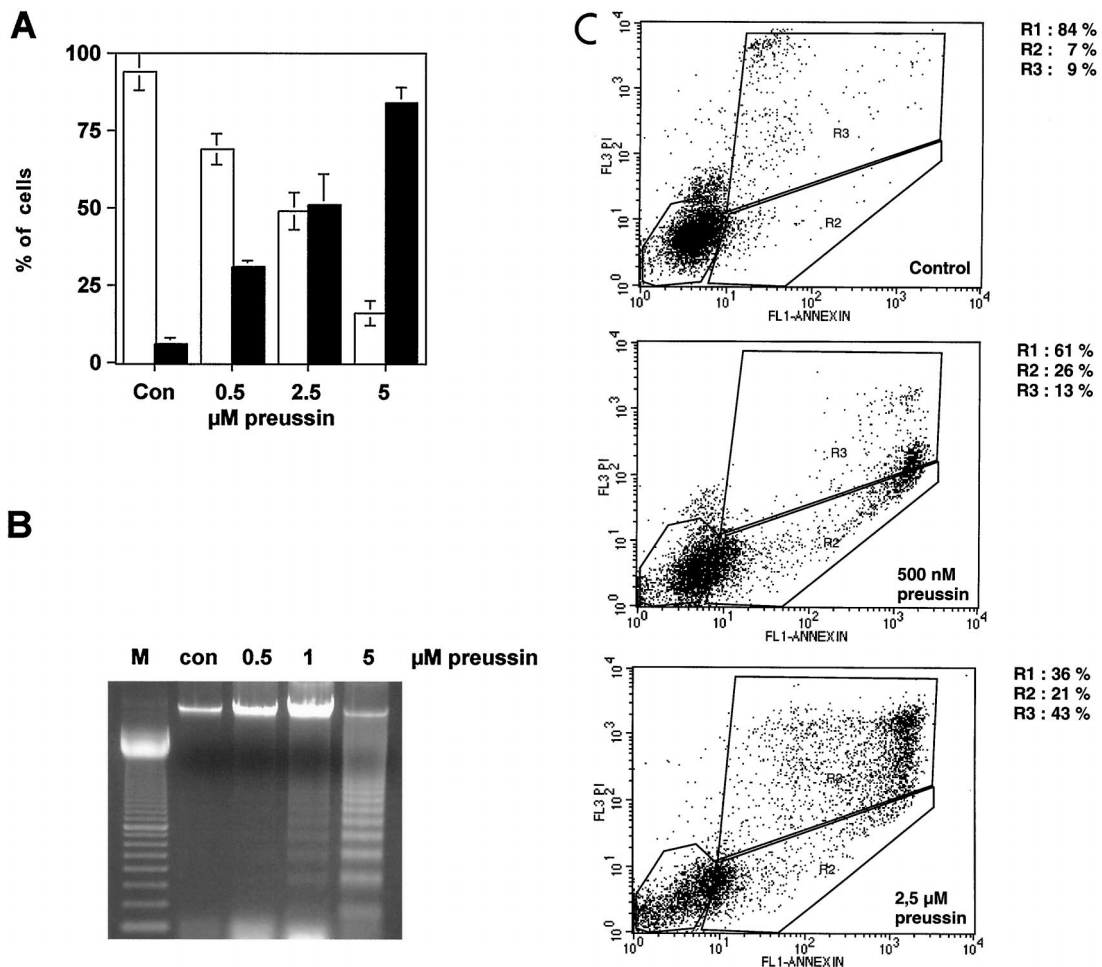


FIG. 7. Induction of apoptosis by preussin in HL-60 cells. (A) Cytological detection of apoptotic cells. HL-60 cells treated with increasing concentration of preussin were stained with Hoechst 33342 and propidium iodide. The percentage of live (□) or apoptotic (■) cells is indicated. (B) DNA fragmentation. The agarose gel shows DNA fragmentation (DNA ladder) in cells that were untreated control [con] or treated with 0.5, 1, or 2.5 μM preussin. A 100-bp ladder was loaded in lane M. (C) Annexin V binding. Untreated cells (Control) and cells treated with 500 nM or 2.5 μM preussin were incubated with fluorescein isothiocyanate-labeled annexin V and propidium iodide; this was followed by FACS analysis. The designated areas represent live cells (R1), annexin V-positive cells (early apoptosis; R2), and propidium iodide-positive cells (late apoptosis and necrosis; R3).

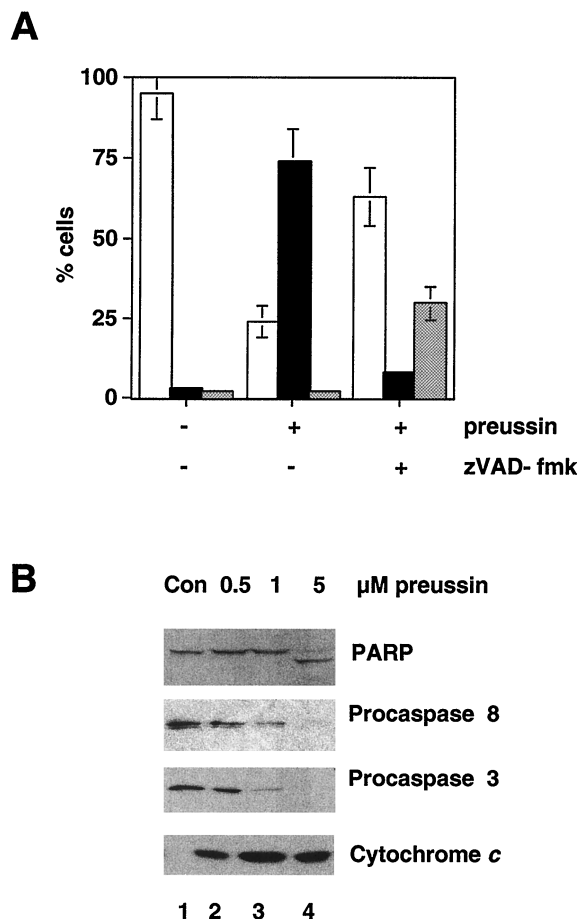


FIG. 8. Role of caspases and cytochrome *c* in the induction of apoptosis by preussin. (A) Effect of caspase inhibition on preussin-induced cell death. HL-60 cells were untreated (-) or treated with preussin (+) after a 1-h preincubation with (+) or without (-) zVAD-fmk (100 μM). The percentage of live (□), apoptotic (■), or necrotic (▨) cells is given. Shown are the average results of three independent experiments ± the standard deviation. (B) Immunoblot analysis of procaspases, PARP, and cytoplasmic cytochrome *c*. Extracts from HL-60 cells that were untreated (Con) or treated with 0.5, 1, or 5 μM preussin for 18 h were analyzed by immunoblotting using antibodies specific for the indicated proteins.

on the cell surface, as detected by annexin V binding. A DNA ladder characteristic of oligonucleosomal DNA fragments was clearly detectable by agarose gel electrophoresis of DNA from HL-60 cells treated with 1 or 5 μM preussin (Fig. 7B). Likewise, FACS analysis of HL-60 cells exposed to 0.5 μM preussin for 18 h showed that 25% of the cells scored positive for annexin V binding (Fig. 7C), which correlates well with the extent of cell killing shown in Fig. 7A. The induction of apoptosis by preussin was also confirmed by terminal deoxynucleotidyltransferase-mediated dUTP-biotin nick endlabeling assay (data not shown).

Caspase activation and cytochrome *c* release in preussin-induced apoptosis. Previous studies have shown that tetrapeptide inhibitors of caspases are capable of inhibiting apoptosis in a variety of systems. To address the role of caspases in preussin-induced apoptosis, HL-60 cells were preincubated for 1 h with zVAD-fmk, a general inhibitor of caspases, before treatment with 5 μM preussin for 18 h. As shown in Fig. 8A, the induction of apoptosis at this time point was largely abrogated by zVAD-fmk, thus indicating an essential role for caspases.

However, zVAD-fmk did not block cell killing completely but rather delayed the onset of death and switched the mechanism of cell death to necrosis (Fig. 8A).

To investigate the involvement of specific caspases, we analyzed extracts from cells treated with 0.5, 1, or 5 μM preussin for 18 h by immunoblotting for procaspases 3 and 8. Cleavage of both proenzymes (Fig. 8B) indicates that caspases 3 and 8 are activated during preussin-induced apoptosis. In agreement with this observation, cleavage of the 116-kDa caspase 3 substrate PARP (21) to the 86-kDa form was also observed (Fig. 8B, top). In addition, cytochrome *c* release from mitochondria was readily detectable (Fig. 8B, bottom). Thus, preussin activates two different apoptotic pathways triggered either by caspase 8 or by cytochrome *c*-caspase 9.

Effect of resistance mechanisms on preussin-induced apoptosis. Another important issue is the question of how drug resistance mechanisms that are commonly found in human tumors affect preussin-induced cell death. Several of the responsive cell lines used in this study lack functional p53, such as HL-60 (44), PC-3, and DU-145 (11) (Fig. 2B), suggesting that the induction of cell death by preussin is p53 independent. We also tested preussin in several human tumor cell lines expressing high levels of Bcl-2, i.e., the small-cell lung carcinoma cell lines SW2 and H69 (Fig. 9A) (46). Whereas preussin

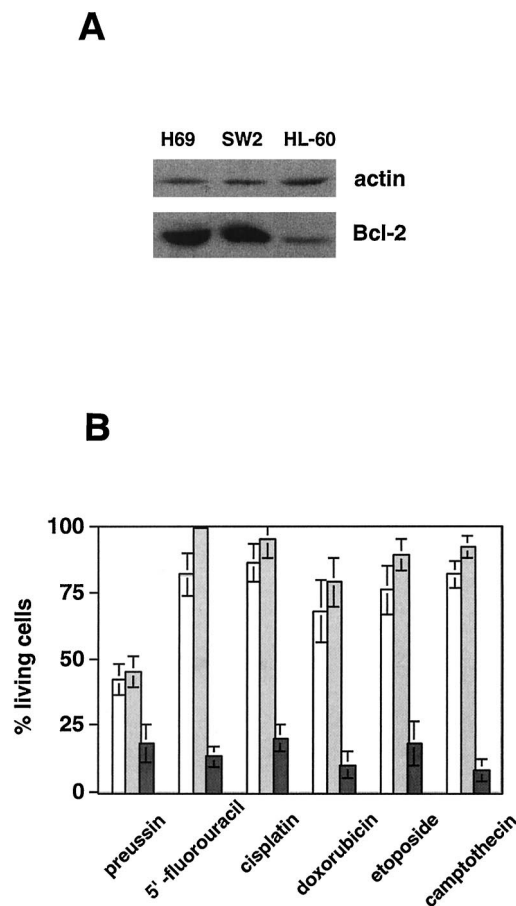


FIG. 9. Induction of cell death by preussin in cells expressing high levels of Bcl-2. (A) Immunoblot analysis of Bcl-2 levels in H69, SW2, and HL-60 cells. The same blot was reprobed with an α-actin antibody as a loading control. (B) Cell killing induced by 10 μM preussin, 500 μM 5'FU, 6 μM Cisp, 1.7 μM Dox, 2 μM Etop, or 500 nM Cam in H69, SW2, and HL-60 cells after 18 h of drug exposure, as determined in Fig. 7A.

- activity of flavone L 86-8275. *Int. J. Oncol.* **6**:31–36.
13. De Azevedo, W. F. J., H. J. Mueller-Dieckmann, U. Schulze-Gahmen, P. J. Worland, E. Sausville, and S. H. Kim. 1996. Structural basis for specificity and potency of a flavonoid inhibitor of human CDK2, a cell cycle kinase. *Proc. Natl. Acad. Sci. USA* **93**:2735–2740.
 14. Evan, G. I., A. H. Wyllie, C. S. Gilbert, T. D. Littlewood, H. Land, M. Brooks, C. M. Waters, L. Z. Penn, and D. C. Hancock. 1992. Induction of apoptosis in fibroblasts by c-myc protein. *Cell* **69**:119–128.
 15. Garrett, M. D., and A. Fattaey. 1999. CDK inhibition and cancer therapy. *Curr. Opin. Genet. Dev.* **9**:104–111.
 16. Gray, N., L. Detivaud, C. Doerig, and L. Meijer. 1999. ATP-site directed inhibitors of cyclin-dependent kinases. *Curr. Med. Chem.* **6**:859–875.
 17. Gray, N. S., L. Wodicka, A.-M. W. H. Thunnissen, T. C. Norman, S. Kwon, F. H. Espinoza, D. O. Morgan, G. Barnes, S. LeClerc, L. Meijer, S.-H. Kim, D. J. Lockhart, and P. G. Schultz. 1998. Exploiting chemical libraries, structure, and genomics in the search for kinase inhibitors. *Science* **281**:533–538.
 18. Hough, M. R., B. N. White, and J. J. Holden. 1988. Tumorigenicity of ten karyotypically distinct cell types present in the human melanoma cell line MeWo-A. *Cancer Genet. Cytogenet.* **32**:117–128.
 19. Hsieh, J. K., S. Fredersdorf, T. Kouzarides, K. Martin, and X. Lu. 1997. E2F1-induced apoptosis requires DNA binding but not transactivation and is inhibited by the retinoblastoma protein through direct interaction. *Genes Dev.* **11**:1840–1852.
 20. Hueber, A. O., and G. I. Evan. 1998. Traps to catch unwary oncogenes. *Trends Genet.* **14**:364–367.
 21. Jänicke, R. U., M. L. Sprengart, M. R. Wati, and A. G. Porter. 1998. Caspase-3 is required for DNA fragmentation and morphological changes associated with apoptosis. *J. Biol. Chem.* **273**:9357–9360.
 22. Johnson, J. H., D. W. Phillipson, and A. D. Kahle. 1989. The relative and absolute stereochemistry of the antifungal agent preussin. *J. Antibiot.* **42**:1184–1185.
 23. Kasahara, K., M. Yoshida, J. Eishima, K. Takesako, T. Beppu, and S. Horinouchi. 1997. Identification of preussin as a selective inhibitor for cell growth of the fission yeast *ts* mutants defective in *Cdc2*-regulatory genes. *J. Antibiot.* **50**:267–269.
 24. Kaur, G., M. Stetler-Stevenson, S. Sebers, P. Worland, H. H. Sedlacek, C. Myers, J. Czech, R. Naik, and E. A. Sausville. 1992. Growth inhibition with reversible cell cycle arrest of carcinoma cells by flavone L86-8275. *J. Natl. Cancer Inst.* **84**:1736–1740.
 25. Kinzler, K. W., and B. Vogelstein. 1994. Cancer therapy meets p53. *N. Engl. J. Med.* **331**:49–50.
 26. Kochi, S. K., and R. J. Collier. 1993. DNA fragmentation and cytolysis in U937 cells treated with diphtheria toxin or other inhibitors of protein synthesis. *Exp. Cell Res.* **208**:296–302.
 27. Korsmeyer, S. J. 1999. BCL-2 gene family and the regulation of programmed cell death. *Cancer Res.* **59**:1693s–1700s.
 28. Losiewicz, M. D., B. A. Carlson, G. Kaur, E. A. Sausville, and P. J. Worland. 1994. Potent inhibition of CDC2 kinase activity by the flavonoid L86-8275. *Biochem. Biophys. Res. Commun.* **201**:589–595.
 29. Müller, D., C. Bouchard, B. Rudolph, P. Steiner, I. Stuckmann, R. Saffrich, W. Ansorge, W. Huttner, and M. Eilers. 1997. Cdk2-dependent phosphorylation of p27 facilitates its Myc-induced release from cyclin E/cdk2 complexes. *Oncogene* **15**:2561–2576.
 30. Parker, B. W., G. Kaur, W. Nieves-Neira, M. Taimi, G. Kohlhagen, T. Shimizu, M. D. Lowiewicz, Y. Pommier, E. A. Sausville, and A. M. Senderowicz. 1998. Early induction of apoptosis in hematopoietic cell lines after exposure to flavopiridol. *Blood* **91**:458–465.
 31. Patel, V., A. M. Senderowicz, D. Pinto, Jr., T. Igishi, M. Raffeld, L. Quintanilla-Martinez, J. F. Ensley, E. A. Sausville, and J. S. Gutkind. 1998. Flavopiridol, a novel cyclin-dependent kinase inhibitor, suppresses the growth of head and neck squamous cell carcinomas by inducing apoptosis. *J. Clin. Investig.* **102**:1674–1681.
 32. Phillips, A. C., S. Bates, K. M. Ryan, K. Helin, and K. H. Vousden. 1997. Induction of DNA synthesis and apoptosis are separable functions of E2F-1. *Genes Dev.* **11**:1853–1863.
 33. Reed, J. 1996. Mechanisms of Bcl-2 family protein function and dysfunction in health and disease. *Behring Inst. Mitt.* **97**:72–100.
 34. Reed, J. C. 1999. Mechanisms of apoptosis avoidance in cancer. *Curr. Opin. Oncol.* **11**:68–75.
 35. Sausville, E. A., D. Zaharevitz, R. Gussio, L. Meijer, M. Louarn-Leost, C. Kunick, R. Schultz, T. Lahusen, D. Headlee, S. Stinson, S. G. Arbuck, and A. Senderowicz. 1999. Cyclin-dependent kinases: initial approaches to exploit a novel therapeutic target. *Pharmacol. Ther.* **82**:285–292.
 36. Schrupp, D. S., W. Matthews, G. A. Chen, A. Mixon, and N. K. Altorki. 1998. Flavopiridol mediates cell cycle arrest and apoptosis in esophageal cancer cells. *Clin. Cancer Res.* **4**:2885–2890.
 37. Schwartz, O., U. Veith, C. Gaspard, and V. Jäger. 1999. Stereoselective synthesis and biological evaluation of anisomycin and 2-substituted analogues. *Synthesis* **1999**:1473–1490.
 38. Schwartz, R. E., J. Liesch, O. Hensens, L. Zitano, S. Honeycutt, G. Garrity, R. A. Fromtling, J. Onishi, and R. Monaghan. 1988. L-657,398, a novel antifungal agent: fermentation, isolation, structural elucidation and biological properties. *J. Antibiot.* **41**:1774–1779.
 39. Senderowicz, A. M., D. Headlee, S. F. Stinson, R. M. Lush, N. Kalil, L. Villalba, K. Hill, S. M. Steinberg, W. D. Figg, A. Tompkins, S. G. Arbuck, and E. A. Sausville. 1998. Phase I trial of continuous infusion flavopiridol, a novel cyclin-dependent kinase inhibitor, in patients with refractory neoplasms. *J. Clin. Oncol.* **16**:2986–2999.
 40. Shapiro, G. I., D. A. Koestner, C. B. Matranga, and B. J. Rollins. 1999. Flavopiridol induces cell cycle arrest and p53-independent apoptosis in non-small cell lung cancer cell lines. *Clin. Cancer Res.* **5**:2925–2938.
 41. Sherr, C. J., and J. M. Roberts. 1999. CDK inhibitors: positive and negative regulators of G₁-phase progression. *Genes Dev.* **13**:1501–1512.
 42. Shimizu, S., Y. Eguchi, W. Kamiike, H. Matsuda, and Y. Tsujimoto. 1996. Bcl-2 expression prevents activation of the ICE protease cascade. *Oncogene* **12**:2251–2257.
 43. Thornberry, N. A., and Y. Lazebnik. 1998. Caspases: enemies within. *Science* **281**:1312–1316.
 44. Wolf, D., and V. Rotter. 1985. Major deletions in the gene encoding the p53 tumor antigen cause lack of p53 expression in HL-60 cells. *Proc. Natl. Acad. Sci. USA* **82**:790–794.
 45. Wright, J., G. L. Blatner, and B. D. Cheson. 1998. Clinical trials referral resource. Clinical trials of flavopiridol. *Oncology (Huntingt.)* **12**:1018–1024.
 46. Ziegler, A., G. H. Luedke, D. Fabbro, K. H. Altmann, R. A. Stahel, and U. Zangemeister-Wittke. 1997. Induction of apoptosis in small-cell lung cancer cells by an antisense oligodeoxynucleotide targeting the Bcl-2 coding sequence. *J. Natl. Cancer Inst.* **89**:1027–1036.
 47. Zwicker, J., and R. Müller. 1997. Cell-cycle regulation of gene expression by transcriptional repression. *Trends Genet.* **13**:3–6.